# The Configurational Space of Rocksalt-Type Oxides for High-Capacity Lithium Battery Electrodes

*Alexander Urban, Jinhyuk Lee, and Gerbrand Ceder**

**A unifying theory is presented to explain the lithium exchange capacity of rocksalt-like structures with any degree of cation ordering, and how lithium percolation properties can be used as a guideline for the development of novel high-capacity electrode materials is demonstrated. The lithium percolation properties of the three most common lithium metal oxide phases, the layered $\alpha$-$NaFeO_2$ structure, the spinel-like LT-$LiCoO_2$ structure, and the $\gamma$-$LiFeO_2$ structure, are demonstrated and a strong dependence of the percolation thresholds on the cation ordering and the lithium content is observed. The poor performance of $\gamma$-$LiFeO_2$-type structures is explained by their lack of percolation of good Li migration channels. The spinel-like structure exhibits excellent percolation properties that are robust with respect to off-stoichiometry and some amount of cation disorder. The layered structure is unique, as it possesses two different types of lithium diffusion channels, one of which is, however, strongly dependent on the lattice parameters, and therefore very sensitive to disorder. In general it is found that a critical Li-excess concentration exists at which Li percolation occurs, although the amount of Li excess needed depends on the partial cation ordering. In fully cation-disordered materials, macroscopic lithium diffusion is enabled by ≈10% excess lithium.**

## 1. Introduction

With increasing demand for portable electronics fueled by lithium ion batteries, the urge for improved battery technology has been rising. The development of high-capacity and high-energy-density cathode materials is generally considered the greatest challenge in the advancement of lithium ion battery technology.[1,2] Today, ordered lithium metal oxides with formula unit $LiMO_2$ (M = metal species), especially layered oxides and ordered spinels, are the most important class of cathode materials for lithium-ion batteries in consumer electronics.[3–6] The configurational space of stoichiometric ordered rocksalt-type lithium metal oxides is already vast, as any combination of redox active metal species and every ordered structure has to be considered. However, the recent discoveries of high-capacity materials with lithium-excess compositions (Li/M ratio greater than 1) indicate that the lithium content and the degree of cation disorder are also important parameters to be optimized.[7–12] In general, very little design guidelines are available to preselect high-capacity electrode materials, and the search for novel cathodes has been largely by trial and error.

Here, we show that there is a well-defined relation between the composition, transition-metal ordering, and the diffusion kinetics of lithium intercalation. Mapping the configurational space of ordered and cation-disordered rocksalt-type lithium metal oxides in terms of their diffusion kinetics leads to design guidelines for potential high-capacity cathode materials. Drawing a connection between the atomistic lithium hopping mechanism and macroscopic lithium diffusion allows us to determine the conditions under which fast lithium diffusion can be expected. Our methodology based on percolation theory is independent of the transition-metal species, and the results of our simulations therefore apply to any general rocksalt-type lithium metal oxide. In addition, it is straightforward to generalize the formalism to different classes of ion conductors, provided that the microscopic migration mechanism of the ions is known.

In the second section, the structure of rocksalt-type lithium metal oxides and the current understanding of lithium migration are briefly reviewed. A relationship between the microscopic hopping mechanism and macroscopic lithium diffusion is established. Percolation theory and the Monte–Carlo formalism used to predict lithium percolation properties are discussed in the third section. In sections 4 and 5, the results of the simulations are presented; we report critical compositions for the three most common ordered phases of lithium metal oxides, both, for the ideal crystal structures and as a function of gradual disordering. Finally, in section 6, we point out how the results of the percolation analyses can be used for engineering high-capacity cathode materials.

## 2. Background: Lithium Percolation Through Rocksalt-type Oxides

The crystal structures of many lithium metal oxides with formula unit $LiMO_2$, where M typically represents one or more metal species, are related to the cubic rocksalt (NaCl) structure: oxygen atoms occupy the sites of a face-centered cubic (FCC) lattice, and the cations (lithium and other metal atoms) occupy

Dr. A. Urban, J. Lee, Prof. G. Ceder
Department of Materials Science and Engineering
Massachusetts Institute of Technology
77 Massachusetts Ave., Cambridge, MA 02139, USA
E-mail: gceder@mit.edu

DOI: 10.1002/aenm.201400478

 © 2014 WILEY-VCH Verlag GmbH & Co. KGaA, Weinheim 

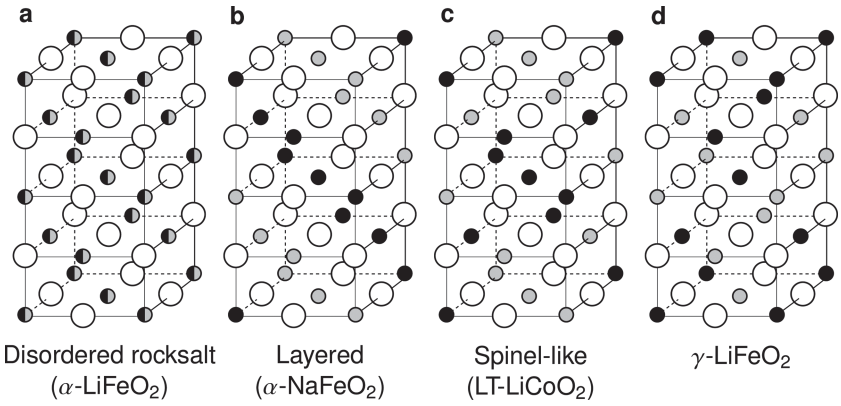


**Figure 1.** The four most common rocksalt-type lithium metal oxide crystal structures: a) disordered rocksalt structure in which all cation sites are equivalent, b) layered structure ($\alpha$-$NaFeO_2$ structure), c) spinel-like low-temperature (LT) $LiCoO_2$ structure, and d) $\gamma$-$LiFeO_2$ structure. Large empty circles indicate oxygen sites, small gray and black filled circles stand for lithium and transition metal sites.

the FCC sub-lattice of octahedral interstices (**Figure 1**a). If all cation sites are equivalent, the disordered-rocksalt ($\alpha$-$LiFeO_2$ or NaCl-type) structure is obtained. Specific cation orderings on their respective sub-lattice result in crystal structures of lower symmetry. The typical cation arrangements observed in $LiMO_2$ structures were reviewed by Hewston and Chamberland[13] and later explained by Wu et al.[14] using atomistic modeling. The most common ordered phases of lithium metal oxides are i) the layered $\alpha$-$NaFeO_2$ structure, in which lithium and transition metal cations segregate into layers in the cubic (111) direction (Figure 1b), ii) the spinel-like low-temperature $LiCoO_2$ structure, and iii) the $\gamma$-$LiFeO_2$ structure (Figure 1c,d).[14] The layered structure is by far the most common, and its stability has been attributed to its ability to independently relax the oxygen octahedra around each type of cation.[14] Hence, it is found when the alkali and metal cations are very different in size, as in $NaFeO_2$ or $LiCoO_2$. The $\gamma$-$LiFeO_2$ cation ordering is the electrostatically favored arrangement, and hence is obtained when the size difference between the cations is small. Another structure, the orthorhombic $LiMnO_2$ ordering, is only observed for the Mn cation and has been attributed to strong magnetic and Jahn-Teller effects.[15,16] This structure will not be further discussed in this article.

### 2.1. Microscopic Diffusion Mechanism vs. Macroscopic Percolation

The cathode material in a lithium-ion battery functions by reversible extraction and re-intercalation of $Li^+$ ions, and hence good lithium transport throughout the bulk of particles is essential in order to achieve high capacity-to-mass and -volume ratios.

To sustain macroscopic ion migration, a cathode material (and generally any ion conductor) has to meet at least two requirements: i) the material has to support facile ion diffusion via low-barrier channels and ii) these diffusion channels need to span the entire structure, or in other words, the diffusion channels need to form a percolating network. Hence, it is not sufficient to consider the microscopic diffusion mechanism alone: even if low-barrier diffusion channels exist, they might not occur in large enough concentration or proper arrangement to support macroscopic lithium migration.

Several studies have found that in rocksalt-type lithium metal oxides, lithium migration between two octahedral sites proceeds via a tetrahedral activated state (o–t–o diffusion), as direct migration through the O–O edge shared by the octahedral sites is too high in energy.[17–20] The activation barrier for this process is mainly determined by the electrostatic repulsion between the tetrahedral activated Li and the species (metal cation or vacancy) on its two face-sharing sites. In the following, we will refer to these two face-sharing sites as gate sites, since they decide whether a diffusion channel is open or closed (**Figure 2**).

In stoichiometric layered lithium metal oxides (Figure 1b), every tetrahedral site is coordinated by either 3 lithium ions and 1 (transition-) metal (TM) ion, or 1 lithium ion and 3 TM ions (**Figure 3**). Only the first of these environments connects at least two lithium sites and can therefore sustain lithium migration. Hence, for each lithium diffusion channel in the layered structure, exactly one gate site is a TM site, while the second one is a lithium site. In this case, extracting the lithium cation from the gate site reduces the activation barrier dramatically, so that a di-vacancy mechanism, involving a vacancy on one of the two gate sites, becomes dominating.[17,18] The barrier for migration of lithium through such a 1-TM channel is correlated with the TM valence and the lithium–TM separation. The latter distance varies with the height of the Li layer, the slab distance, as it constrains how far the TM can relax away when lithium enters the activated state.[21] Typical slab distances in layered cathode materials are between 2.6 and 2.7 Å (**Table 1**), which results in activation barriers well below 500 meV.[21] All lithium sites in stoichiometric layered materials are equivalent, and hence all sites are interconnected by 1-TM channels and form a two-dimensional percolating network inside of the lithium slabs.

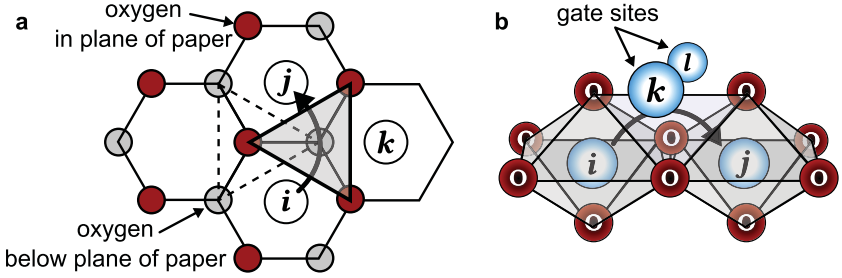


**Figure 2.** Schematics of the diffusion from octahedral lithium site *i* to site *j*. a) Top view in rocksalt (111)-direction. Large empty circles denote octahedral sites. The arrow indicates one of two lithium diffusion channels that connect sites *i* and *j*. Only one gate site, *k*, is depicted. b) 3D view of the same diffusion channel along with both gate sites, *k* and *l*. The di-vacancy lithium diffusion mechanism requires one of the gate sites to be vacant.


© 2014 WILEY-VCH Verlag GmbH & Co. KGaA, Weinheim

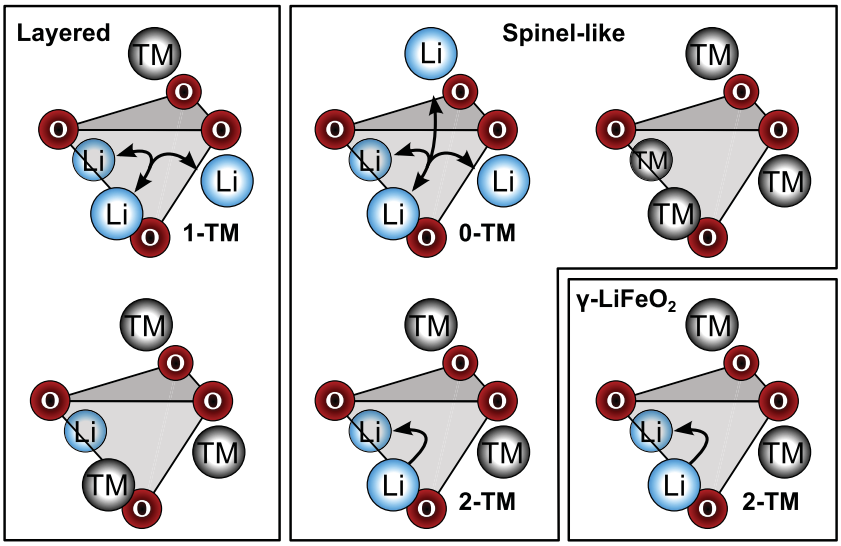


**Figure 3.** Cation distributions around tetrahedral sites in the stoichiometric ordered lithium transition-metal oxides of Figure 1. Potential lithium diffusion channels are indicated with arrows.

Note that migration barriers associated with 1-TM diffusion channels vary upon delithiation: first, because of the increasing electrostatic repulsion while the transition metal cations are oxidized to higher valence, and second, because of the change of the slab distance. During charge, the lithium slab initially widens as the electrostatic attraction between the lithium and oxygen atoms decreases, but at the end of charge, when most of the lithium has been extracted, a collapse of the lithium slab is observed that results in a dramatic decrease of the lithium mobility.[22–24]

The cation distribution in the stoichiometric spinel-like (LT-$LiCoO_2$) structure (Figure 1c) is the result of the perfect segregation into tetrahedral lithium and TM clusters. Three different cation arrangements around tetrahedral sites are present in the structure, with lithium-to-transition metal ratios (Li:TM) equal to 4:0 (only lithium), 0:4 (only TM), and 2:2 (Figure 3). Each two neighboring octahedral lithium sites in the spinel-like structure are connected by one 0-TM channel, whose two gate sites are lithium sites, and one 2-TM channel, whose gate sites are TM sites. Due to the low repulsion between the activated lithium ion and lithium/vacancies on the gate sites, 0-TM channels are active irrespective of the size of the diffusion channel.[12,19,25] In addition, the activation barrier for the diffusion through a 0-TM channel is relatively independent of the transition metal species in the material, as no TM is near the activated state. The spinel-like structure possesses a percolating network of 0-TM lithium diffusion channels and therefore supports macroscopic lithium migration.

Finally, in the stoichiometric $\gamma$-$LiFeO_2$ structure (Figure 1d) only 2-TM diffusion channels exist (Figure 3). However, the 2-TM channels are generally inactive, as two TM ions exert a strong electrostatic repulsion on the activated tetrahedral lithium ion. The high lithium diffusion barriers in the $\gamma$-$LiFeO_2$ structure have been demonstrated computationally for lithiated anatase ($LiTiO_2$) by Belak, Wang, and van der Ven.[26] Hence, the $\gamma$-$LiFeO_2$ structure does not generally support macroscopic lithium migration.

### 2.2. Cation Disorder

In contrast to the ordered crystal phases discussed so far, in the disordered rocksalt structure (Figure 1a), the local environment around lithium sites and diffusion channels is stochastic and follows a normal distribution. All lithium diffusion channel types (0-TM, 1-TM, and 2-TM) occur in cation-disordered structures. As argued above, 2-TM channels are generally inactive. It remains to determine, whether 1-TM channels can support macroscopic lithium migration in cation-disordered structures, or if only 0-TM channels are available.

Recall that in layered materials the activation barrier associated with 1-TM channels critically depends on the slab distance. Due to the higher valence and smaller ionic radius of transition metal cations compared to lithium cations, even a few percent of cation disorder can result in a dramatic decrease of the lithium slab distance in layered structures.[34,35] For a number of materials a reduction of cation mixing has been observed to

**Table 1.** Slab distances $d_{slab}$ in representative layered lithium transition metal oxides, and lattice constants $a$ and tetrahedron heights $h_{tet} = \frac{a}{\sqrt{3}} h_{tet} = \frac{a}{\sqrt{3}}$ for a number of cation-disordered materials with disordered-rocksalt crystal structure. Lattice parameters taken from the original publications (column "Ref."). The tetrahedron height in disordered rocksalts is equivalent to the slab distance in layered materials.

| Layered oxides | | | Cation-disordered oxides | | | |
|---|---|---|---|---|---|---|
| Material | $d_{slab}$ [Å] | Ref. | Material | $a$ [Å] | $h_{tet}$ [Å] | Ref. |
| $LiNiO_2$ | 2.602(3) | [27] | $LiTiO_2$ | 4.149(1) | 2.395(4) | [28] |
| $LiCoO_2$ | 2.637(4) | [29] | $LiMnO_2$ | 4.179(4) | 2.412(9) | [28] |
| $LiVO_2$ | 2.640(4) | [30] | $\alpha$-$LiFeO_2$ | 4.157(1) | 2.400(1) | [13] |
| $LiMoO_2$ | 2.695(1) | [31] | $Li_{0.542}Co_{1.458}O_2$ | 4.143(2) | 2.392(0) | [28] |
| | | | $Li_{0.8388}Ni_{1.1612}O_2$ | 4.074(1) | 2.352(1) | [28] |
| | | | $LiNi_{0.5}Ti_{0.5}O_2$ | 4.1453(6) | 2.3933(2) | [32] |
| | | | $LiCo_{0.5}Ti_{0.5}O_2$ | 4.14 | 2.39 | [33] |


© 2014 WILEY-VCH Verlag GmbH & Co. KGaA, Weinheim

result in improved energy density.[35–38] The $c/a$ lattice parameter ratio, which measures the slab distance relative to the oxygen distance around the TM layer, has indeed been used in patents and publications to indicate the quality of materials in terms of their electrochemical activity.[34,39–42]

In fully cation-disordered materials, the distinction between lithium and transition metal slabs is no longer valid, and no unique slab distance can be defined. Instead, the average height of tetrahedral sites may be used as a generalized geometric criterion.[12] For the disordered-rocksalt structure the tetrahedron height $h_{tet}$ is proportional to the lattice constant $a$ and is given as $h_{tet} = \frac{a}{\sqrt{3}}$. Typical tetrahedron heights in cation-disordered structures are 2.35–2.45 Å, which is much smaller than typical slab distances in layered structures (Table 1). As this small tetrahedron height limits how far the gate-TM can move when lithium is in the activated state, it results in energy barriers above 500 meV for lithium migration through 1-TM channels.[12,21] Most 1-TM channels can therefore be considered inactive in cation-mixed materials, and thus only 0-TM channels can sustain lithium migration.

In general, if a rocksalt-type lithium metal oxide possesses a percolating network of 0-TM channels it will support macroscopic lithium diffusion irrespective of its cation ordering. Layered materials are an exception, as their large lithium slab distances enable migration through 1-TM channels.

### 2.3. Excess Lithium

Since 0-TM channels imply a local lithium-rich domain, their concentration will increase with increasing lithium content. In stoichiometric rocksalt-type lithium transition metal oxides with formula unit $LiTMO_2$ the molar ratio of lithium to transition metal is 1:1. In that composition, every TM cation carries a formal charge of 3+, and upon lithium deintercalation during the charging of the battery the transition metal is gradually oxidized from TM(3+) to TM(4+). In order to introduce excess lithium, i.e., to increase the Li:TM ratio beyond 1, higher valent transition metal cations need to be introduced to satisfy the charge balance. In principle, a larger-than-stoichiometric lithium content leads to a larger theoretical specific capacity of the cathode, provided that the TM species can exchange more than one electron. In recent years several promising lithium-excess cathode materials have been suggested in the literature.[9,43,44]

Variable lithium content and multiple transition metal species result in a very large composition space for off-stoichiometric materials. Our aim is to determine the lithium contents at which a percolating 0-TM network is formed, so as to define clearer boundaries of this vast composition space that can be used to engineer new materials.

## 3. Percolation Theory

Given an infinite lattice whose sites are randomly occupied with probability $x$; what is the critical concentration $x = x_c$ such that an infinite spanning network of occupied sites exists, if bonds are formed between nearest neighbor sites? This is the site percolation problem of percolation theory.[45–48] The probability $p_s$ that a spanning network exists on an infinite lattice is a step function

$$p_s(x) = \begin{cases} 0 \text{ if } x < x_c \\ 1 \text{ if } x > x_c \end{cases} \quad (1)$$

with a discontinuity at the critical concentration $x_c$, the percolation threshold. While analytic values for the site percolation threshold of many 2D lattices have been derived (see for example ref. [47], approximations for 3D lattices have to be obtained from Monte–Carlo simulations.[49,50] Such numerical simulations usually impose periodic boundary conditions, for which $p_s(x)$ is replaced by the probability $p_w(x)$ that a periodically wrapping network exists. Due to finite-size effects, the periodic wrapping probability is not a step function but sigmoidal and approaches $p_s(x)$ asymptotically with increasing size of the simulation cell. **Figure 4**a shows the convergence of $p_w(x)$ towards $p_s(x)$ for supercells of the FCC primitive unit cell. As can be seen from the graph, the inflection point of $p_w(x)$ is not sensitive with respect to the supercell size and coincides with the percolation threshold, which allows an accurate approximation of $x_c = 0.199$ despite the periodic boundary conditions (reference value for FCC: $x_c = 0.1994(2)$).[49]

The second quantity from percolation theory that is of interest in the following sections is the fraction $P$ of sites that are part of the infinite percolating network. Assuming a single periodically wrapping cluster, at concentrations $x > x_c$ each occupied site belongs either to the percolating network or to a finite isolated cluster. In numerical simulations, $P$ is available as the ratio of the number of sites in the periodically wrapping cluster $N_{wrap}$ and the total number of sites $N_{sites}$

$$P(x) = \frac{N_{wrap}(x)}{N_{sites}} \quad (2)$$

With increasing concentration the number of sites in the wrapping cluster approaches the number of occupied sites, i.e., less and less sites belong to isolated clusters and $P\ (x > x_c) \approx x$ (Figure 4b).

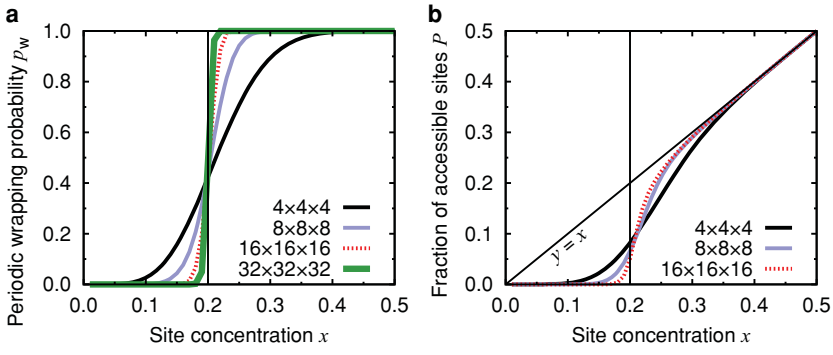


**Figure 4.** Convergence of a) the periodic wrapping probability and b) the fraction of accessible sites with the size of the simulation cell. The different curves correspond to FCC supercells ranging from $4 \times 4 \times 4$ primitive cells (64 sites) to $32 \times 32 \times 32$ cells (32 768 sites). The vertical line at $x \approx 0.2$ indicates the percolation threshold $x_c$.


© 2014 WILEY-VCH Verlag GmbH & Co. KGaA, Weinheim

To apply percolation theory to lithium migration through different types of diffusion channels, we need to extend the concept of site percolation beyond the simple nearest-neighbor model discussed above. Instead, we consider two lithium sites $i$ and $j$ (on the FCC sublattice of cations) to be connected only if an active diffusion channel between these sites exists. In that case, the percolating network will only consist of lithium sites that are interconnected by active diffusion channels, and the ratio $P(x)$ of Equation (2) corresponds to the amount of lithium (usually in atoms per formula unit) that becomes accessible at a certain lithium content $x$. Only accessible lithium, i.e., those lithium atoms that can be reversible extracted and re-intercalated, contribute to the electrochemical capacity. In practice, the accessible lithium content is therefore more readily comparable to experimental results than the percolation threshold.

### 3.1. Monte–Carlo Percolation Simulations

We performed Monte–Carlo simulations to determine the percolation threshold, Equation (1), and the accessible lithium content, Equation (2), for different cases of active lithium diffusion channels. The possible scenarios are: i) only 0-TM channels are active, ii) 1-TM and 0-TM channels are active, and iii) all channels, 0-TM, 1-TM, and 2-TM, are active. Case (iii) simply corresponds to a nearest neighbor site percolation model, as two neighboring lithium sites are always connected by either a 0-TM, 1-TM, or 2-TM channel. For scenarios (i) and (ii) the species on the gate sites need to be considered. Mind that each two octahedral lithium sites $i$ and $j$ are connected by two potential tetrahedral diffusion channels (Figure 2) due to the edge-sharing nature of the octahedral sites in rocksalt-type structures; in scenario (ii), i.e., with active 1-TM channels, $i$ and $j$ will be connected, if any of the four gate sites belonging to those two channels is a lithium site. When only 0-TM channels are active, both gate sites of at least one of the two channels need to be lithium sites. Hence, our approach is to decorate the FCC lattice of cation sites with lithium or TM, according to some prescribed composition and state of order, and code each diffusion channel as active or inactive based on which of the above scenarios we are considering. We then evaluate whether the active channels are percolating.

In the MC simulations, a cluster of sites is considered to be periodically wrapping in one dimension if it contains two different periodic images of the same lithium site.[51] The comparison of the translation vectors of the periodic images allows furthermore to detect the dimensionality of the percolating network.

Following the methodology by Newman and Ziff,[51] at the beginning of each MC sweep $i$, all cation sites are occupied by transition metal ions. Then, at each step one randomly selected TM is replaced by lithium. When the new lithium site results in a wrapping lithium cluster, the current concentration $x_c^{(i)}$ is stored. The MC sweep continues until all TM ions have been converted to lithium, while at each step for $x > x_c^{(i)}$ the number of sites within the percolating cluster, $N_{wrap}^{(i)}(x)$, are stored. After $N_{MC}$ MC sweeps, the percolation threshold is estimated as

$$x_c = \frac{1}{N_{MC}} \sum_{i}^{N_{MC}} x_c^{(i)} \tag{3}$$

where the cumulative distribution function of $x_c^{(i)}$ is the periodic wrapping probability, and the accessible lithium content is given by

$$P(x) = \frac{1}{N_{sites} N_{MC}} \sum_{i}^{N_{MC}} N_{wrap}^{(i)}(x) \tag{4}$$

The MC simulations discussed in this work comprised $N_{MC} = 1000$ MC sweeps to guarantee well-converged results. Each cation ordering defines two distinct sublattices for lithium ions and TM ions, respectively. The impact of long-range cation ordering on the critical lithium contents was modeled by analyzing the percolation on the lithium sublattice first, before including the transition-metal sublattice in the simulation: 1) at the beginning of the simulation all sites of both sublattices are decorated with TM ions. 2) At each MC step one random TM ion on the lithium sublattice is converted to lithium, and the structure is screened for percolating clusters. 3) Only after all sites of the lithium sublattice have been converted to lithium, does the simulation continue with the sites of the TM sublattice.

Cation disorder was introduced in a similar fashion: instead of beginning the simulation with the lithium sublattice sites of the stoichiometric ordered material, before each MC sweep a number of lithium and TM sites are randomly interchanged. A fully disordered structure is obtained when half of the sites of the TM sublattice are interchanged with half of the sites of the lithium sublattice. Every arbitrary degree of cation disorder can be simulated by interchanging smaller numbers of TM and lithium sites.

## 4. Lithium Percolation in Disordered-Rocksalt Materials

**Figure 5** shows the periodic wrapping probability and the accessible lithium content in fully cation-disordered lithium transition metal oxides for the three different scenarios of active diffusion channels discussed in Section 3.1: i) assuming all lithium diffusion channels (0-TM, 1-TM, and 2-TM) are active, ii) only channels that support the di-vacancy mechanism, i.e., 1-TM and 0-TM channels, and iii) only 0-TM channels. Note that the unit of the abscissa in Figure 5 and all following figures has been converted from concentration to lithium contents per formula unit, which is a more common notation in electrochemistry. Since a lithium concentration of 1 corresponds to 2 lithium atoms per $Li_xTM_{2-x}O_2$ formula unit, the actual value of the percolation threshold for case (i) is twice the one of Figure 4. The percolation threshold for a network of active 1-TM and 0-TM lithium diffusion channels lies with $x_c = 0.662$ atoms per formula unit clearly below the stoichiometric composition ($x = 1$). However, when only 0-TM channels are considered active, 9% excess lithium is required to achieve percolation, as the critical concentration is raised to $x_c = 1.092$. Even more than 25% excess lithium ($x = 1.257$ atoms per formula unit) is required for 1 lithium


© 2014 WILEY-VCH Verlag GmbH & Co. KGaA, Weinheim

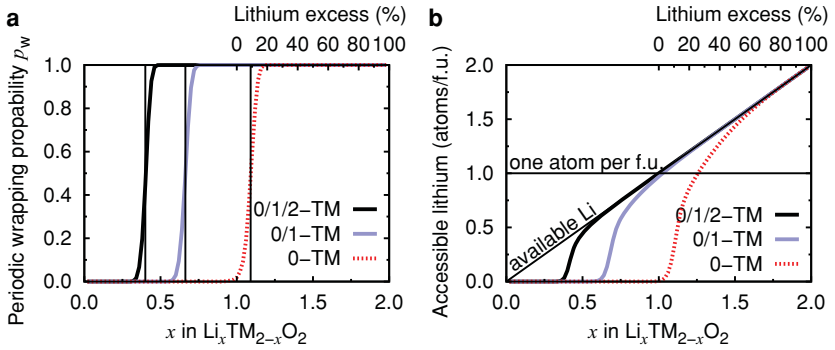


**Figure 5.** a) Periodic wrapping probabilities and percolation thresholds (indicated by vertical bars) in disordered rocksalt-type structures for the various possible combinations of active diffusion channels discussed in the text. If only 0-TM channels are active, percolation requires around 10% excess lithium. b) Accessible amount of lithium as function of the overall lithium content. More than 25% lithium excess is required to extract one lithium atom per formula unit (f.u.) based on 0-TM diffusion. Both, the wrapping probabilities and the accessible lithium content were computed for the $16 \times 16 \times 16$ supercell of Figure 4.

atom per formula unit to become accessible by 0-TM migration (Figure 5b).

As argued in Section 2.1, most 1-TM diffusion channels are inactive in cation-disordered materials, and a percolating network of 0-TM channels would be required to utilize such materials. Hence, the results from the percolation simulation are in agreement with the experimental observation that stoichiometric cation-disordered materials possess only a negligible reversible capacity. However, the simulations also show that excess lithium will enable 0-TM percolation in cation-disordered materials. Indeed, disordered $Li_{1.211}Mo_{0.467}Cr_{0.3}O_2$ (23.3% lithium excess, but with slight lithium deficiency) exhibits a large reversible capacity,[12] and other electrochemically active disordered lithium excess materials have been reported.[52–55]

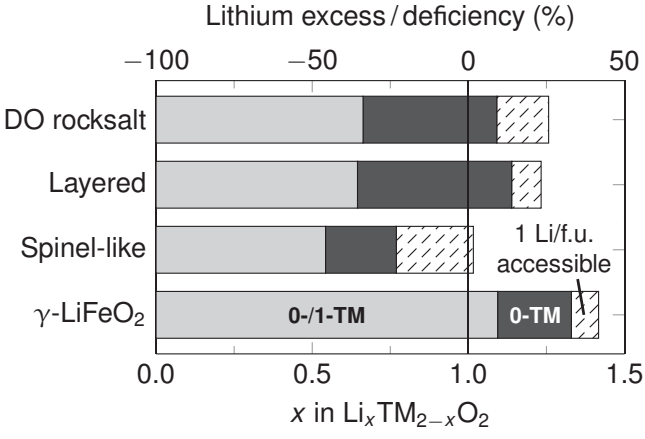


**Figure 6.** Critical lithium concentrations for different lithium-rich and lithium-deficient ordered structures (also see Figure 1). The first gray region of the bars indicates the percolation threshold if 0-TM and 1-TM channels are active. The black region is the extra lithium required to achieve percolation if only 0-TM are active. The third hatched region gives the lithium content that is required to enable extraction of one lithium atom per formula unit (f.u.) $Li_xTM_{2-x}O_2$ based on 0TM migration.

## 5. Lithium Percolation in Ordered Crystal Phases

Employing the modified MC algorithm of Section 3.1, the percolation properties of cation-ordered crystal phases were analyzed. A graphical comparison of the critical concentrations for the different cation orderings of Figure 1 is shown in **Figure 6**, and the numerical values are listed in **Table 2**. Interestingly, the percolation thresholds for the layered cation ordering are within 4% of the values found for cation-disordered materials. Although, the critical lithium content for 0-TM percolation (black bars in Figure 6) is slightly larger in layered materials, the extraction of 1 lithium atom per formula unit requires nearly identical lithium excess (red bars in Figure 6). Hence, layered materials would not offer any topological advantage over cation-disordered structures, if their 1-TM channels were not active. Yet, very different results are found for the Spinel-like and $\gamma$-$LiFeO_2$ structures.

The topological analysis of cation distributions in Section 2.1 already informed us that the stoichiometric spinel-like structure is 0-TM percolating. Indeed, the result of the percolation simulation shows that the structure becomes 0-TM percolating for lithium contents as low as $x = 0.77$ atoms per formula unit, which translates to 23% lithium deficiency compared to the stoichiometric composition. These remarkable percolation properties may be responsible for the fact that lithium oxides with spinel-like structure readily deintercalate lithium and can be used not only as cathode materials,[5,6,56] but also, in delithiated form, as lithium insertion anode in lithium ion batteries.[4,57,58] Our results also indicate that the excellent performance of spinel-related materials is remarkably tolerant to off-stoichiometry. Note that the tetrahedral site of a 0-TM channel may become more stable for lithium than its surrounding octahedral sites once all but one lithium ions have been extracted from its face-sharing sites,[59] as is the case in the $LiM_2O_4$ (= $Li_{0.5}MO_2$) spinel structure. Consequently, the lithium migration mechanism may locally change to tetrahedral–octahedral–tetrahedral. Since the diffusion path remains unchanged (i.e., the same sites are visited during lithium diffusion), the percolation model does not need to be adjusted to account for this effect.

**Table 2.** Critical lithium contents $x$ per formula unit $Li_xM_{2-x}O_2$ for lithium diffusion under different open channel scenarios (top row). The last column contains the lithium contents required for the extraction of one Li atom per formula unit via 0-TM diffusion. All numbers are based on MC simulations of $16 \times 16 \times 16$ FCC supercells. See also Figure 6 for a graphical representation of some of the data.

| | 0-/1-/2-TM | 0-/1-TM | 0-TM only | 1 Li acc. |
|---|---|---|---|---|
| DO-rocksalt | 0.398 | 0.662 | 1.092 | 1.257 |
| Layered | 0.432 | 0.644 | 1.138 | 1.233 |
| Spinel-like | 0.390 | 0.542 | 0.770 | 1.016 |
| $\gamma$-$LiFeO_2$ | 0.428 | 1.094 | 1.330 | 1.417 |


© 2014 WILEY-VCH Verlag GmbH & Co. KGaA, Weinheim

As discussed in Section 2.1, the stoichiometric γ-$LiFeO_2$ structure only possesses 2-TM channels, and is therefore neither 0-TM nor 1-TM percolating. A very large amount of more than 40% lithium excess ($x$ = 1.42 atoms, Table 2) is required to render one lithium atom per formula unit 0-TM accessible. To the authors' knowledge, no functioning lithium electrode material with γ-$LiFeO_2$ structure is known, consistent with our prediction.

### 5.1. Cation Mixing in Ordered Materials

Perfectly disordered structures and perfectly ordered structures are merely the limits of a large possible configurational space of cation arrangements, and it is important to understand the opportunities to create partially disordered structures with good percolation properties. **Figure 7** shows the 0-TM percolation threshold in the three cation ordered phases of Figure 1 as function of the cation mixing. Cation disorder was introduced as described in Section 3.1. In the spinel-like and γ-$LiFeO_2$ structures, the percolation threshold initially changes nearly linearly towards the value in the disordered phase with increasing degree of cation mixing. This is not the case for the layered structure, in which the percolation threshold is minimal for around 50% cation mixing. The trends are similar but slightly less pronounced for the amount of 0-TM accessible lithium. The minimal excess lithium content (22%) in the layered structure to extract one lithium atom per formula unit is achieved for around 24% cation disorder. In general, the critical percolation concentrations of the ordered phases converge rapidly to those of the disordered system above 75% cation mixing, which indicates that the remaining correlation between cation sites has only a negligible influence on percolation.

## 6. Discussion and Implications

In essence, the geometry of lithium diffusion through rocksalt-type lithium TM oxides creates three types of diffusion channels that are associated with the local distribution of cations around tetrahedral sites: 0-TM, 1-TM, and 2-TM channels. Not only the arrangement of these channels throughout the structure, but also their size, is critical for good diffusivity. In general, 2-TM channels exhibit a very high lithium diffusion barrier and do not contribute to macroscopic lithium migration. 1-TM channels are only active when their tetrahedron height is sufficiently large, whereas 0-TM channels are not sensitive with respect to the local structural environment and are usually active. Ordered $LiMO_2$ crystal structures can be classified by their distribution of diffusion channel types: the γ-$LiFeO_2$ structure only possesses 2-TM channels, and is therefore unsuitable as a lithium ion conductor. In the ideal α-$NaFeO_2$ (layered) structure the cation ordering results in a 2D percolating network of 1-TM channels that are, in the absence of cation mixing, large enough to support lithium diffusion. The ideal situation is found for the spinel-like LT-$LiCoO_2$ ordering, which gives rise to a perfect segregation of lithium cations into 0-TM channels. Finally, the disordered-rocksalt (α-$LiFeO_2$) structure possesses a

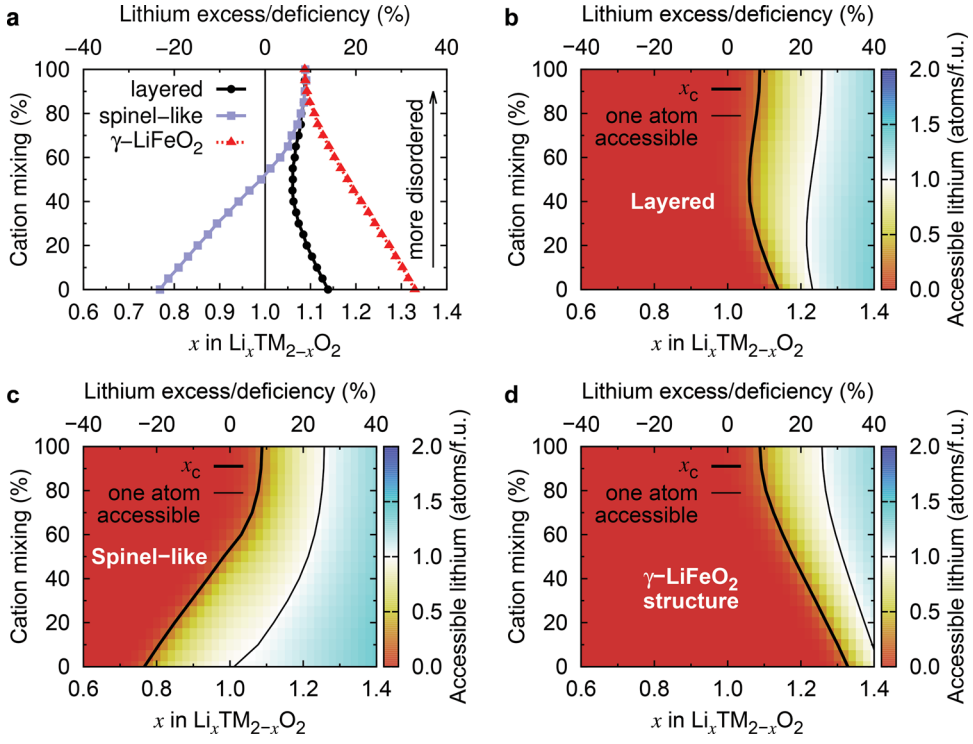


**Figure 7.** a) Critical lithium concentrations for 0-TM percolation and b,c) 0-TM accessible lithium atoms per formula unit as function of the overall lithium content and the degree of cation mixing in the three cation-ordered phases of Figure 1, layered, spinel-like, and γ-$LiFeO_2$. The structure specific percolation thresholds are indicated by thick black contour lines. Compositions falling into the region left of these contour lines are not 0-TM percolating. Thin lines indicate the compositions at which one lithium atom per formula unit becomes 0-TM accessible.


© 2014 WILEY-VCH Verlag GmbH & Co. KGaA, Weinheim

normal distribution of all diffusion channel types, from which only 0-TM channels are active. However, in stoichiometric cation-disordered structures with Li/TM ratio of 1, the 0-TM channels are not percolating. Our simulations of off-stoichiometric compositions show that excess lithium is required for all but the spinel-like structure to become 0-TM percolating. The high concentration of 0-TM channels in the spinel-like ordering permits 0-TM percolation in compounds with more than 20% lithium deficiency, whereas around 10% of lithium excess is required in the layered and the disordered-rocksalt structure, and even more than 30% is needed to make the $\gamma$-$LiFeO_2$ structure percolating.

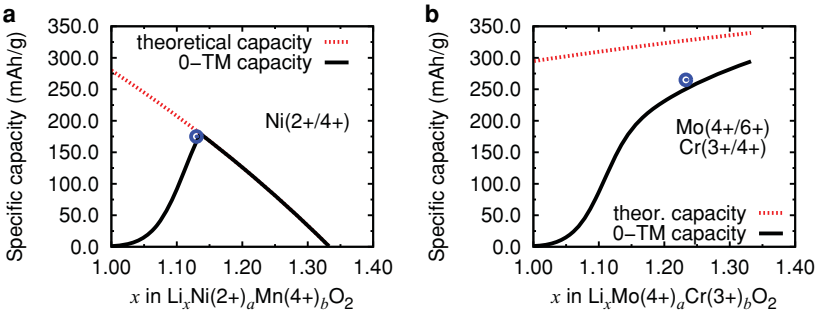


**Figure 8.** Maximum theoretical specific capacity (dotted line) and 0-TM capacity (solid line) based on the disordered-rocksalt structure for a) Li(Li,Ni,Mn)$O_2$ and b) Li(Li,Cr,Mo)$O_2$. The observed capacities at empirically optimized compositions are indicated by circles (data from ref. [61,12]).

These insights should spur the development of novel materials: i) in layered materials lithium excess can make 0-TM channels available, when cation mixing occurs and closes the 1-TM channels. Currently, lithium-excess layered materials are of considerable interest,[7–9] and it is not clear whether these diffuse lithium through 1-TM channels, 0-TM channels, or a combination thereof. ii) The creation of novel materials along the spectrum between fully ordered and disordered structures may have additional benefits: for disordered $Li_{1.211}Mo_{0.467}Cr_{0.3}O_2$ virtually no change of the lattice parameters has been observed during charge/discharge,[12] thus the variation in the tetrahedron heights is minimal and almost no change in the lithium migration barrier has to be expected during delithiation and lithium re-intercalation.[21] Such zero strain materials are critical for applications in solid state batteries, in which volume changes of the electrodes will result in breaking of the solid-electrolyte interface. Indeed, one of the reasons why the theoretical capacity of layered materials can not be achieved is the very large change of the lattice parameters and concomitant slab-space reduction when a large amount of lithium is extracted. This reduces the lithium mobility sharply,[17,19] and hence lithium can not be extracted. It is therefore not surprising that high-capacity materials exhibit some degree of disorder,[9,12,60] as the disorder mitigates the slab-distance contraction at high states of charge.

The percolation analysis presented in this work is completely independent of the transition metal species and can be applied to any arbitrary compound. Given an actual composition, the 0-TM accessible lithium content directly translates to a 0-TM specific capacity. Only lithium sites that are directly connected to the percolating 0-TM network contribute to the 0-TM capacity. However, lithium atoms that are separated from the 0-TM network by only a few 1-TM channels may be accessible as well, depending on the material-specific 1-TM diffusion barriers. Since 0-TM channels are active irrespective of the transition metal species and are not particularly sensitive with respect to the lattice parameters, the 0-TM capacity can be understood as a conservative estimate of the reversible specific capacity. Whether the true specific capacity lies closer to the 0-TM estimate or to the maximum theoretical capacity will be determined by the amount of active 1-TM diffusion channels, which exhibit a strong structural dependence. Two examples of lithium-excess compounds from the literature[12,61] are shown in **Figure 8**. The experimentally optimized capacities of both materials falls indeed in the expected range and coincides, in the case of Li(Li,Mn,Ni)$O_2$, with the predicted maximal 0-TM capacity. In addition to an estimate of the optimal lithium content, systematic doping strategies for existing materials can be developed by considering the effect of reducing or increasing the degree of cation disorder.

## 7. Conclusion

In this work we mapped the configurational space of common lithium metal oxide crystal phases to determine bounds on the composition of high-capacity electrode materials. Based on percolation theory, we explained the lithium diffusion properties of layered and spinel-like materials, and pointed out the reasons why materials with $\gamma$-$LiFeO_2$ structure are not suitable as electrode materials. We showed that cation disorder is not detrimental for layered materials, provided a sufficient amount (≈20%) of excess lithium is present in the composition. Indeed, some degree of disorder is argued to deliver beneficial materials properties, such as negligible strain upon charge/discharge. Our analysis is purely based on the crystal topology, and hence is not specific to any metal cation species. The results give rise to a general understanding of lithium migration that provides guidelines for the engineering of novel high-capacity and high-energy-density electrode materials.

## Acknowledgments

This work was supported by the Robert Bosch Corporation, by Umicore Specialty Oxides and Chemicals, by a Samsung Scholarship (J.L.), and by the Assistant Secretary for Energy Efficiency and Renewable Energy, Office of Vehicle Technologies of the U.S. Department of Energy under Contract No. DE-AC02–05CH11231, under the Batteries for Advanced Transportation Technologies (BATT) Program subcontract #7056411. Computational resources from the National Energy Research Scientific Computing Center (NERSC) and from the Extreme Science and Engineering Discovery Environment (XSEDE) are gratefully acknowledged. The authors thank Xin Li for valuable discussions.

Received: March 19, 2014
Revised: April 19, 2014
Published online: May 11, 2014


© 2014 WILEY-VCH Verlag GmbH & Co. KGaA, Weinheim

[1] M. S. Whittingham, *Chem. Rev.* **2004**, *104*, 4271.
[2] J. B. Goodenough, Y. Kim, *Chem. Mater.* **2010**, *22*, 587.
[3] K. Mizushima, P. Jones, P. Wiseman, J. Goodenough, *Mater. Res. Bull.* **1980**, *15*, 783.
[4] T. Ohzuku, A. Ueda, N. Yamamoto, *J. Electrochem. Soc.* **1995**, *142*, 1431.
[5] M. Thackeray, P. Johnson, L. de Picciotto, P. Bruce, J. Goodenough, *Mater. Res. Bull.* **1984**, *19*, 179.
[6] K. M. Shaju, P. G. Bruce, *Dalton Trans.* **2008**, *40*, 5471.
[7] C. S. Johnson, M. M. Thackeray, in Interfaces, Phenomena, and Nanostructures in Lithium Batteries, *Electrochem. Soc. Proc.* **2000**, *36*, 47.
[8] Z. Lu, D. D. MacNeil, J. R. Dahn, *Electrochem. Solid-State Lett.* **2001**, *4*, 191.
[9] M. M. Thackeray, S.-H. Kang, C. S. Johnson, J. T. Vaughey, R. Benedek, S. A. Hackney, *J. Mater. Chem.* **2007**, *17*, 3112.
[10] R. Wang, X. He, L. He, F. Wang, R. Xiao, L. Gu, H. Li, L. Chen, *Adv. Energy Mater.* **2013**, *3*, 1358.
[11] X. Yu, Y. Lyu, L. Gu, H. Wu, S.-M. Bak, Y. Zhou, K. Amine, S. N. Ehrlich, H. Li, K.-W. Nam, X.-Q. Yang, *Adv. Energy Mater.* **2014**, *4*, 1300950.
[12] J. Lee, A. Urban, X. Li, D. Su, G. Hautier, G. Ceder, *Science* **2014**, *343*, 519.
[13] T. Hewston, B. Chamberland, *J. Phys. Chem. Solids* **1987**, *48*, 97.
[14] E. J. Wu, P. D. Tepesch, G. Ceder, *Philos. Mag. Part B* **1998**, *77*, 1039.
[15] G. Ceder, S. K. Mishra, *Electrochem. Solid-State Lett.* **1999**, *2*, 550.
[16] S. K. Mishra, G. Ceder, *Phys. Rev. B* **1999**, *59*, 6120.
[17] A. Van der Ven, G. Ceder, *Electrochem. Solid-State Lett.* **2000**, *3*, 301.
[18] A. Van der Ven, G. Ceder, *J. Power Sources* **2001**, *97*, 529.
[19] A. Van der Ven, J. Bhattacharya, A. A. Belak, *Acc. Chem. Res.* **2013**, *46*, 1216.
[20] M. S. Islam, C. A. J. Fisher, *Chem. Soc. Rev.* **2014**, *43*, 185.
[21] K. Kang, G. Ceder, *Phys. Rev. B* **2006**, *74*, 094105.
[22] G. G. Amatucci, J. M. Tarascon, L. C. Klein, *J. Electrochem. Soc.* **1996**, *143*, 1114.
[23] A. Van der Ven, M. K. Aydinol, G. Ceder, *J. Electrochem. Soc.* **1998**, *145*, 2149.
[24] G. Ceder, A. Van der Ven, M. K. Aydinol, *J. Mater.* **1998**, *50*, 35.
[25] J. Bhattacharya, A. Van der Ven, *Phys. Rev. B* **2011**, *83*, 144302.
[26] A. A. Belak, Y. Wang, A. Van der Ven, *Chem. Mater.* **2012**, *24*, 2894.
[27] A. Hirano, R. Kanno, Y. Kawamoto, Y. Takeda, K. Yamaura, M. Takano, K. Ohyama, M. Ohashi, Y. Yamaguchi, *Solid State Ionics* **1995**, *78*, 123.
[28] M. Obrovac, O. Mao, J. Dahn, *Solid State Ionics* **1998**,*112*, 9.
[29] J. Akimoto, Y. Gotoh, Y. Oosawa, *J. Solid State Chem.* **1998**, *141*, 298.
[30] L. Cardoso, D. Cox, T. Hewston, B. Chamberland, *J. Solid State Chem.* **1988**, *72*, 234.
[31] D. Mikhailova, N. N. Bramnik, K. G. Bramnik, P. Reichel, S. Oswald, A. Senyshyn, D. M. Trots, H. Ehrenberg, *Chem. Mater.* **2011**, *23*, 3429.
[32] S. Prabaharan, M. Michael, H. Ikuta, Y. Uchimoto, M. Wakihara, *Solid State Ionics* **2004**, *172*, 39.
[33] M. Yang, X. Zhao, Y. Bian, L. Ma, Y. Ding, X. Shen, *J. Mater. Chem.* **2012**, *22*, 6200.
[34] Y.-M. Choi, S.-I. Pyun, S.-I. Moon, *Solid State Ionics* **1996**, *89*, 43.
[35] K. Kang, Y. S. Meng, J. Bréger, C. P. Grey, G. Ceder, *Science* **2006**, *311*, 977.
[36] A. Rougier, I. Saadoune, P. Gravereau, P. Willmann, C. Delmas, *Solid State Ionics* **1996**, *90*, 83.
[37] A. Rougier, P. Gravereau, C. Delmas, *J. Electrochem. Soc.* **1996**, *143*, 1168.
[38] Z. Lu, D. D. MacNeil, J. R. Dahn, Electrochem. *Solid-State Lett.* **2001**, *4*, 200.
[39] C. Delmas, I. Saadoune, A. Rougier, *J. Power Sources* **1993**, *44*, 595.
[40] T. Ohzuku, Y. Makimura, *Chem. Lett.* **2001**, *30*, 744.
[41] Y. Makimura, T. Ohzuku, *J. Power Sources* **2003**, *119*, 156.
[42] G. Ceder, K. Kang (Massachusetts Institute of Technology), US Patent 8 529 800, **2013**.
[43] Z. Lu, J. R. Dahn, *J. Electrochem. Soc.* **2002**, *149*, 815.
[44] C. Johnson, J.-S. Kim, C. Lefief, N. Li, J. Vaughey, M. Thackeray, *Electrochem. Commun.* **2004**, *6*, 1085.
[45] D. Stauffer, A. Aharony, *Introduction to Percolation Theory*, Taylor & Francis, Philadelphia, PA **1994**.
[46] R. Ewing, A. Hunt, *Percolation Theory for Flow in Porous Media, Lecture Notes in Physics*, Springer, Berlin Heidelberg **2009**, p. 771.
[47] M. B. Isichenko, *Rev. Mod. Phys.* **1992**, *64*, 961.
[48] J. W. Essam, *Rep. Prog. Phys.* **1980**, *43*, 833.
[49] S. C. van der Marck, *Int. J. Mod. Phys. C* **1998**, *09*, 529.
[50] C. D. Lorenz, R. M. Ziff, *Phys. Rev. E* **1998**, *57*, 230.
[51] M. E. J. Newman, R. M. Ziff, *Phys. Rev. Lett.* **2000**, *85*, 4104.
[52] C. Delmas, S. Brèthes, M. Ménétrier, *J. Power Sources* **1991**, *34*, 113.
[53] C. Delmas, H. Cognac-Auradou, J. M. Cocciantelli, M. Ménétrier, J. P. Doumerc, *Solid State Ionics* **1994**, *69*, 257.
[54] C. Delmas, H. Cognac-Auradou, *J. Power Sources* **1995**, *54*, 406.
[55] V. Pralong, V. Gopal, V. Caignaert, V. Duffort, B. Raveau, *Chem. Mater.* **2012**, *24*, 12.
[56] T. Ohzuku, S. Takeda, M. Iwanaga, *J. Power Sources* **1999**, *81*, 90.
[57] E. Ferg, R. J. Gummow, A. de Kock, M. M. Thackeray, *J. Electrochem. Soc.* **1994**, *141*, 147.
[58] M. M. Thackeray, *J. Electrochem. Soc.* **1995**, *142*, 2558.
[59] J. Bhattacharya, A. Van der Ven, *Phys. Rev. B* **2010**, *81*, 104304.
[60] Y. S. Meng, G. Ceder, C. P. Grey, W.-S. Yoon, M. Jiang, J. Bréger, Y. Shao-Horn, *Chem. Mater.* **2005**, *17*, 2386.
[61] S.-T. Myung, S. Komaba, N. Kumagai, *Solid State Ionics* **2004**, *170*, 139.

 © 2014 WILEY-VCH Verlag GmbH & Co. KGaA, Weinheim 